*molecules*

MDPI

*Communication*

# Conjugated Diphenylaniline-Azulene Co-Oligomers with Intense Absorption and Emission in the Visible Region

**Nurlan Merkhatuly [1,*], Amantay Iskanderov [1,*], Saltanat Abeuova [2], Ablaykhan Iskanderov [1] and Saltanat Zhokizhanova [3]**

[1] Laboratory of Organic Semiconductor Chemistry, Karaganda Buketov University, Karaganda 100028, Kazakhstan; org.semicond@yandex.kz
[2] The Higher School of Natural Sciences, Astana International University, Astana 020000, Kazakhstan; abeuova.salta@gmail.com
[3] Department of Physics and Chemistry, Saken Seifullin Kazakh Agro Technical Research University, Astana 010011, Kazakhstan; saltanat_zh75@mail.ru
* Correspondence: nurlanmerhatuly@mail.ru (N.M.); dr.amantay@ya.ru (A.I.)

**Abstract:** New conjugated 2,6-diphenylaniline-azulene co-oligomers of linear and branched structure were synthesized by the interaction of borylazulenes with diphenylaniline bromides under Suzuki–Miyaura cross-coupling conditions. The obtained diphenylaniline-azulene co-oligomers intensively absorb and emit visible light (410–700 nm region); in particular, they exhibit strong emissions in the green, as well as orange, range, with maxima of 510/590 nm. It is shown that such properties appear as a result of the positive resonance exposure to aniline fragments significantly rearranging the electronic structure of azulene, in particular, the levels and energy gaps of frontal HOMO–LUMO orbitals.

**Keywords:** azulene; diphenylaniline-azulene; conjugated azulene co-oligomers; cross-coupling; electron spectra; fluorescence

check for updates

**Citation:** Merkhatuly, N.; Iskanderov, A.; Abeuova, S.; Iskanderov, A.; Zhokizhanova, S. Conjugated Diphenylaniline-Azulene Co-Oligomers with Intense Absorption and Emission in the Visible Region. *Molecules* **2024**, *29*, 5041. https://doi.org/10.3390/molecules29215041

Academic Editors: Shiyong Liu, Guangfu Liao and Jiabin Qiu

Received: 4 October 2024
Revised: 23 October 2024
Accepted: 23 October 2024
Published: 25 October 2024

**Copyright:** © 2024 by the authors. Licensee MDPI, Basel, Switzerland. This article is an open access article distributed under the terms and conditions of the Creative Commons Attribution (CC BY) license (https://creativecommons.org/licenses/by/4.0/).

## 1. Introduction

New strategies for the development of functional materials are of the considerable interest in the dynamics of the development of electronic devices (organic light-emitting diodes, organic field-effect transistors, dye-sensitized organic solar cells, and others) [1,2].

Here, research focuses on the production and use of various molecules (building blocks) that are able to correctly debug the electronic structure of substances to improve and increase the performance of devices.

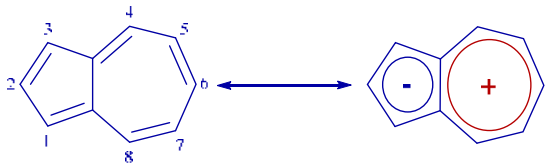
To date, the most effective molecules as building blocks are aromatic hydrocarbons, for example, azulenes.

Azulenes, as non-alternant aromatic compounds, have been the objects of a lot of scientific research over the past few decades [3–11].

Currently, azulene, due to its potential, is widely studied as a functional material for conducting oligomers and polymers, organic light-emitting diodes and other organic semiconductor devices [12–23].

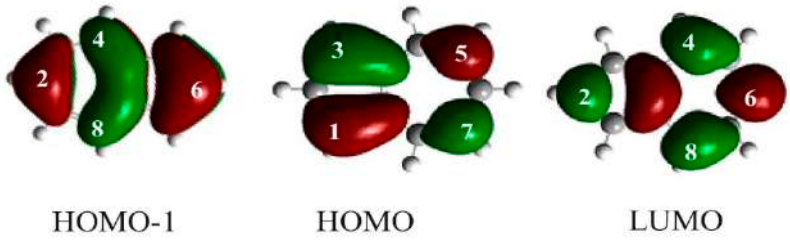
Such interest in them was caused by the dipole structure (μ = 1.08 D) [24] and unusual optical properties, including $S_2 \rightarrow S_0$ anti-Kasha fluorescence [25–29].

Azulene consists of negatively charged five-membered and positively charged seven-membered cycles (Figure 1a). This kind of structure gives high HOMO energy levels and low LUMO energies compared to conventional aromatic compounds [30–34]. In addition, the C-1 and C-3 carbon atoms have high HOMO ratios, and the C-2 and C-6 atoms have high HOMO-1 and LUMO ratios (Figure 1b) [30–33]. Azulene is also blue-colored compared to the colorless isomer naphthalene and shows absorption in the visible region of the spectrum at 580 nm (intensity is only 350 $M^{-1}$ $cm^{-1}$) caused by the forbidden transition $S_0 \rightarrow S_1$ [34].




**1**

**(a).**




**(b).**

**Figure 1.** (**a**) Azulene **1** structure. (**b**) Frontal molecular orbitals **1**.

Thus, it is expected that the introduction of donor diphenylaniline groups at the C-2 and C-6 positions of azulene can lead to a new advanced functional material.

In this work, we report the synthesis with high yields of new conjugated 2,6-diphenylaniline-azulene co-oligomers of linear and branched structures **6** and **8**, via the Suzuki−Miyaura reaction.

## 2. Results and Discussion

Synthetic pathways leading to conjugated diphenylaniline-azulene co-oligomers of linear and branched structures, 6,6-Bis(N,N-diphenylaniline)-2,2-(4-(diphenylamino)phenyl)-bis-azulene **6** and 6,6,6-tris(N,N-diphenylaniline)-2,2,2-(4-(triphenylamino)-tris-azulene **8**, are shown in Schemes 1 and 2.

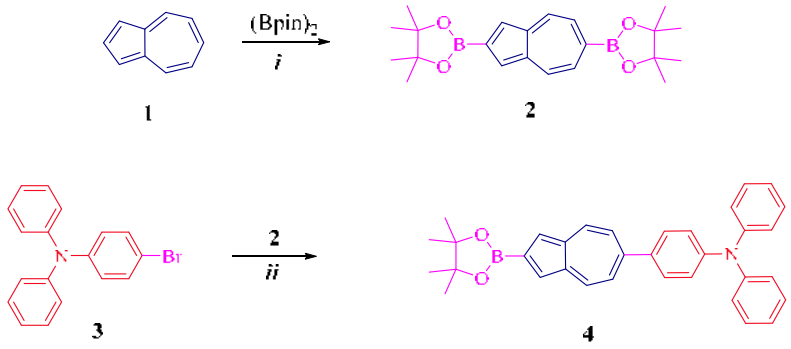
As can be seen from Scheme 1, diborylazulene **2** was obtained by reacting **1** with Bis(pinacolato)diboron in the presence of $[IrCl(cod)]_2$, according to the literature procedure [35]. Then, the coupling of amine **3** with borylazulene **2** (1:3 ratio) in the presence of a $Pd(PPh_3)_2CI_2$ catalyst gives the key compound 2-boryl-6-diphenylaniline-azulene **4** in a high yield of 70%. As can be seen from this scheme, the reaction proceeds regioselectively at the **6** position of the seven-membered azulene ring (Figure S1, Supplementary Materials).

Further, as shown in Scheme 2, the linear co-oligomer bis-azulene **6** was synthesized in a high yield of 76% by reacting dibromotriphenylamine **5** with three equivalents of 2-borylazulene **4** under Suzuki–Miyaura reaction conditions. The expanded tris-azulene **8** co-oligomer was also prepared in a high yield of 72% under similar conditions by reacting tris(4-bromophenyl)amine **7** with four equivalents of 2-borylazulene **4.**

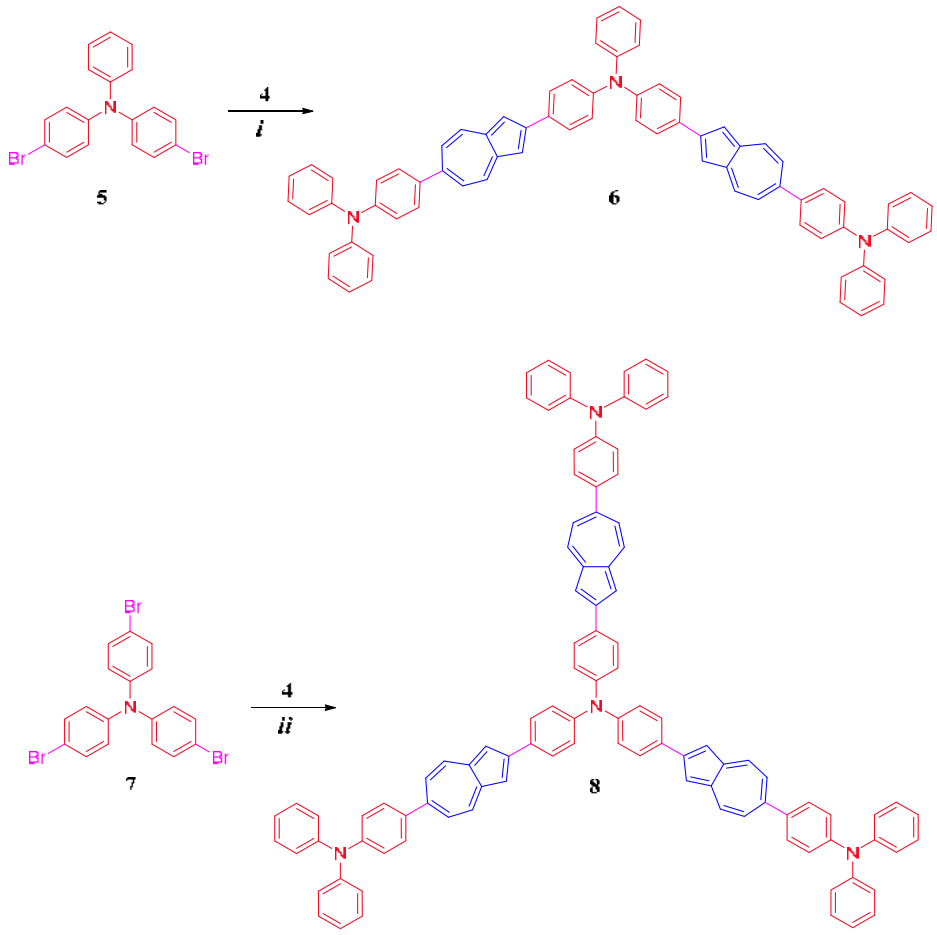
The resulting co-oligomers **6** and **8** are stable brown solids (as opposed to the blue color of the initial azulene). They dissolve well at a temperature of 18–24 °C in solvents such as toluene, chlorobenzene, and methylene chloride.

The structure and purity of the synthesized co-oligomers, 6,6-Bis(N,N-diphenylaniline)-2,2-(4-(diphenylamino)phenyl)-bis-azulene **6** and 6,6,6-tris(N,N-diphenylaniline)-2,2,2-(4-(triphenylamino)-tris-azulene **8**, are determined with spectroscopic methods (Supplementary Materials).

The thermal stability of co-oligomers **6** and **8** was investigated by thermogravimetric analysis ($N_2$ medium, heating 10 °C per minute). The onset of degradation **6** and **8** was recorded at 436 and 425 °C, respectively, showing good thermal stability (Figure S7, Supplementary Materials). Differential scanning calorimetry measurements for **6** and **8** were performed at a scan rate of 10 °C per minute. No endothermic or exothermic transitions were observed over the entire scan range (Figure S8, Supplementary Materials).




**Scheme 1.** Synthesis **4**: (*i*) $[IrCl(cod)]_2$, 2,2′-bipyridine, cyclohexane, reflux, yield 50%; (*ii*) $Pd(PPh_3)_2CI_2$, THF:water (4:1), 75–80 °C, 70%.




**Scheme 2.** Synthesis of **6** and **8**: (*i*) $Pd(PPh_3)_2CI_2$, THF: water (4:1), 75–80 °C, 76%; (*ii*) $Pd(PPh_3)_2CI_2$, THF: water (4:1), 75–80 °C, 72%.

Figure 2 shows the UV–visible absorption spectra of **6** and **8** (Table 1) in comparison with azulene **1**. It can be seen that co-oligomer **6** exhibits an intense visible absorption band with $\lambda_{max}$ at 430 nm ($\varepsilon$ = 22,447 $M^{-1}$ $cm^{-1}$). The edge of the absorption spectrum **6** is at 475 nm, which corresponds to an optical band gap of 2.61 eV.

Co-oligomer **8** also exhibits an intense visible band $\lambda_{max}$ at 465 nm and $\varepsilon$ = 24,621 $M^{-1}$ $cm^{-1}$ (Table 1), which is bathochromically shifted at 35 nm and has a higher intensity than that of **6**. The edge of the absorption spectrum **8** is observed at 490 nm, which corresponds to an optical band gap of 2.53 eV (Figure 2).

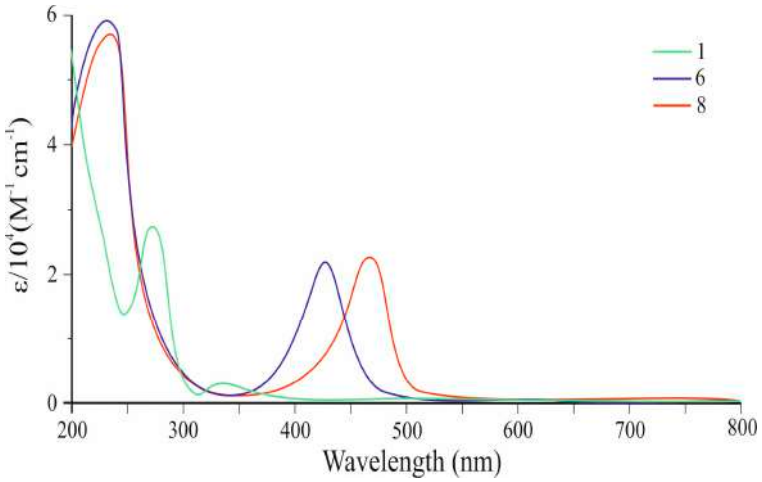



**Figure 2.** UV–vis spectra of co-oligomers **6** and **8**, as well as azulene **1**.

This bias is a consequence of the elongation of the π,π-conjugation (Figure 3) and the reduction in the HOMO–LUMO energy gap. It can be seen that the visible electron absorbances of co-oligomers **6** (ε = 22,447 $M^{-1}$ $cm^{-1}$) and **8** (ε = 24,621 $M^{-1}$ $cm^{-1}$) are stronger than those of **1** (ε = 350 $M^{-1}$ $cm^{-1}$) [34].

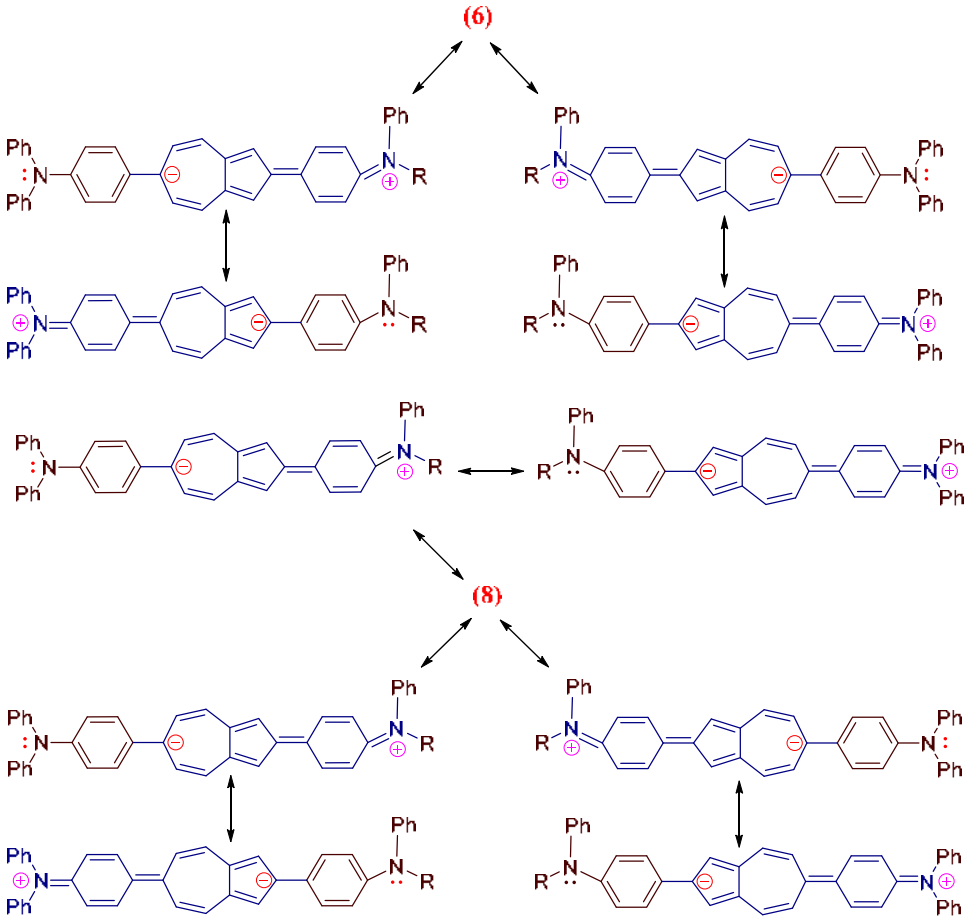



**Figure 3.** Scheme of resonance structures of co-oligomers **6** and **8**.

The electronic absorptions of co-oligomers **6** and **8** in a thin film (Supplementary Materials) were also investigated. As can be seen in Figure S9, the absorption spectra of **6** and **8** in the UV–vis region in spin-coated films (Figure S9a) had a similar appearance

to those in the solution (Figure S9b or Figure 2), but the absorptions in the visible region (λmax at 444 and 483 nm, respectively) are shifted by about 14 and 18 nm to the long-wave length region compared to the solution. This red shift may be caused by intermolecular interactions of the compounds in the solid state.

The absorption wavelengths (380–610 nm) of diphenylaniline-azulene co-oligomers **6** and **8** are comparable to those of a number of applied functional materials, such as oligothiophenes and indophenines [34–42].

**Table 1.** Electronic absorption and fluorescence values of co-oligomers **6** and **8** (C = 1 × $10^{-4}$ in DCM).

| Co-Oligomers | Absorption Data | | Fluorescence Data [a] | |
|---|---|---|---|---|
| | Absorption Maximum (nm) | Molar Coefficient ($M^{-1}$ $cm^{-1}$) | Emission Maximum (nm) | QY, % [b] |
| 6 | 227<br>430 | 58,826<br>22,447 | 510 | 56 |
| 8 | 235<br>465 | 57,881<br>24,621 | 590 | 65 |

[a] $\lambda_{ex}$ (excitation wavelength) 420 nm. [b] QY is fluorescence quantum yield and was measured according to the standard procedure; a dilute solution of 1,4-bis- (5-phenyloxazol-2-yl) benzene in ethanol was used as a standard material [42].

Figure 4 shows the fluorescence spectra of co-oligomers **6** and **8** (values are given in Table 1). Co-oligomer **6** shows a new intense visible band with a maximum at 510 nm (PLQY of 56%) (when excited at 420 nm) (Table 1). Co-oligomer **8**, when excited also at 420 nm, exhibits intense emission at 590 nm (PLQY of 65%) (Table 1). Figure 4 shows that the emission band of **8** is strongly bathochromically shifted at 80 nm with increasing intensity compared to that of co-oligomer **6** (Table 1). We believe that the significant shift in the fluorescence band **8** is the result of the elongation of the conjugation (Figure 3) and the decrease in the gap between HOMO and LUMO. The resulting ability of co-oligomers **6** and **8** to emit intensively in the green, as well as orange, range is unique due to the absence of such in azulene 1.

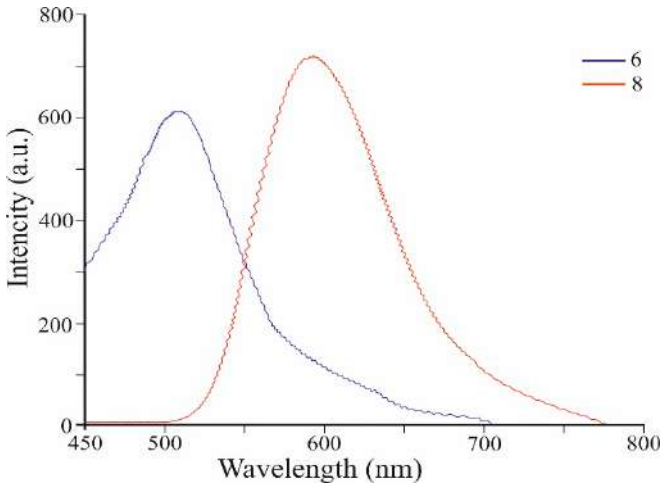



**Figure 4.** Fluorescence spectra of co-oligomers **6** and **8**.

Figure 5 shows the frontal molecular orbitals of co-oligomers **6** and **8** compared to the azulene 1 orbitals obtained by the DFT B3LYP/6- 31G * (Supplementary Materials) method.

It can be seen from this figure that the HOMO orbitals of co-oligomers **6** and **8** are distributed over the skeleton of the entire molecule. This is possible only as a result of the interaction between the HOMO-1 of the azulene cycle and the HOMO of the diphenylaniline fragment [0], since in the HOMO, the C-2 and C-6 atoms of azulene are in the nodal plane, while in the HOMO-1, they have large atomic-orbital coefficients (Figure 1b). It is also

shown that in co-oligomers **6** (−4.65 eV) and **8** (−4.57 eV), HOMOs are located higher in level, and LUMOs are lower (−2.02 eV) than the frontal molecular orbitals of the initial azulene **1** (while the gap between HOMO and LUMO decreases by 0.73 eV and 0.81 eV, respectively). This is due to a change in the order of MO levels between initial compound **1** and co-oligomers **6** and **8** [43]. As a result, the prohibited electronic transition of HOMO → LUMO azulene is enabled [43] and, as a result, leads to strong visible absorption and emission. This is what is observed in the electron and fluorescence spectra of co-oligomers **6** and **8** (Figures 2 and 4).

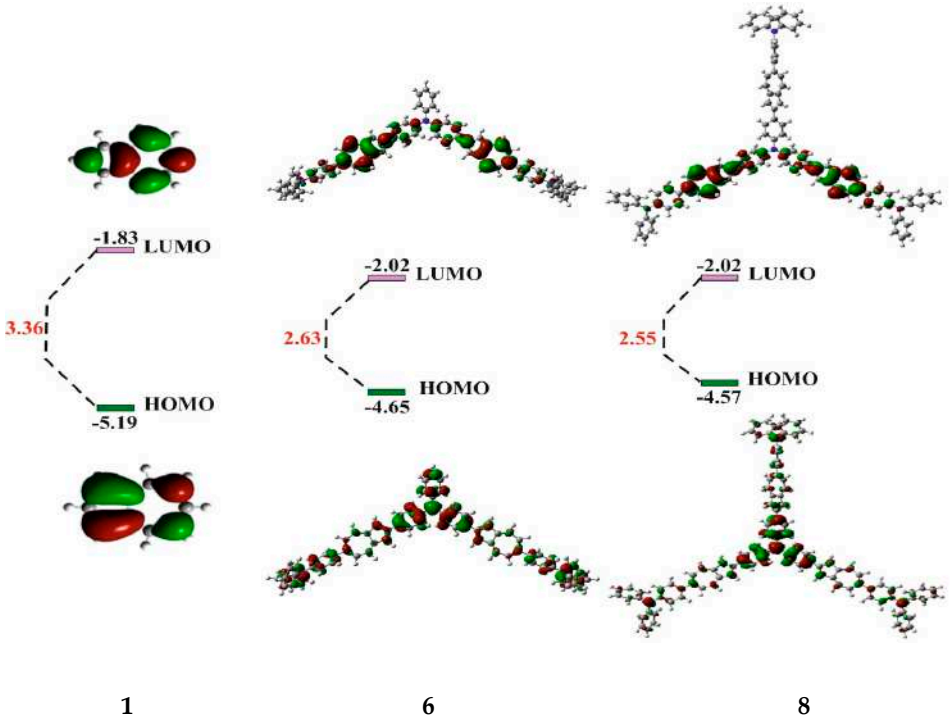



**Figure 5.** Frontal molecular orbitals of co-oligomers **6** and **8** and initial **1**.

Figure 6 shows the redox properties of co-oligomers **6** and **8** investigated by cyclic voltammetry (CV) (Supplementary Materials).

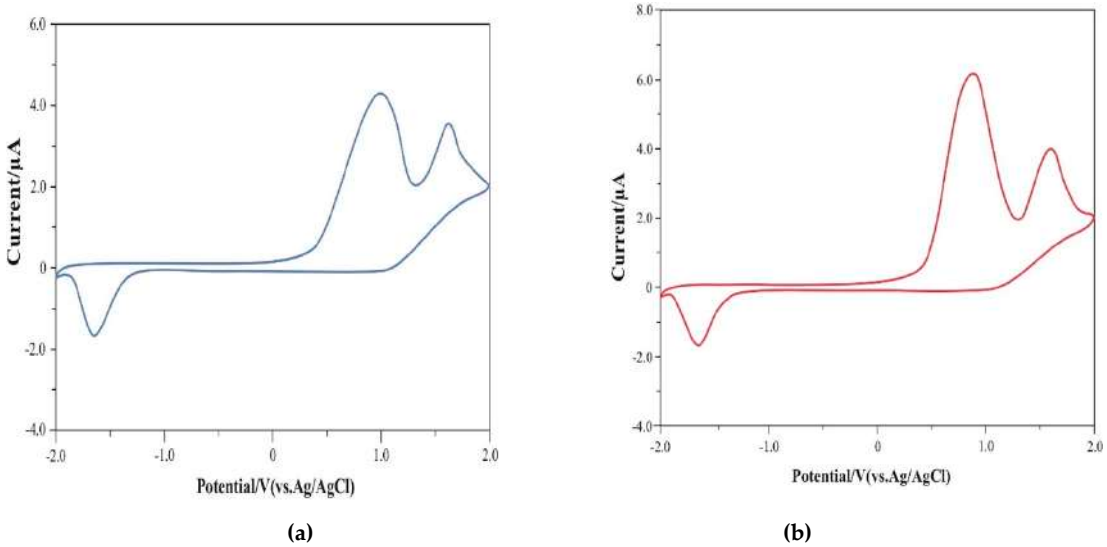



**Figure 6.** CV of co-oligomers (**a**) **6** and (**b**) **8**.

As can be seen, co-oligomer **6** exhibits irreversible oxidation waves at 1.0 V and 1.62 V and irreversible reduction at −1.70 V. Co-oligomer **8** also exhibits irreversible oxidation waves at 0.86 V and 1.66 V and irreversible reduction waves at −1.68 V.

In co-oligomer **6**, the onset of oxidation is observed at 0.38 V and reduction at −1.48 V. Based on these data, the energy levels of HOMO and LUMO **6** are −4.82 eV and −2.92 eV, respectively. Similarly, in co-oligomer **8**, the onset of oxidation is observed at 0.39 V and reduction at −1.46 V, which leads to the following levels of HOMO and LUMO: −4.81 eV and −2.94 eV, respectively.

The energy levels of frontal MO were calculated using the formula given in [44].

It is important to note that the HOMO energy levels of co-oligomers **6** and **8** obtained from the experimental electrochemical studies are close to those calculated via the DFT method (Figure 5), while the calculated values of the LUMO levels differ slightly from the experimental ones (the discrepancy is approximately 0.90 V and 0.92 V, respectively).

## 3. Materials and Methods

The following methods were used in the work: For NMR spectrometry, a JNM-ECA 500 spectrometer (Jeol, Tokyo, Japan) (operating frequencies 500 MHz for $^{1}$H and 126 MHz for $^{13}$C; solvent $CDCl_3$, internal standard TMS) was used; for FT-IR spectrometry, an Avatar-360 in KBr (Thermo Nicolet, Waltham, MA, USA) was used; for HRMS spectrometer, UV–vis spectra **6** and **8** were Thermo Electron Corporation DFS (Thermo Fisher Scientific Inc., Waltham, MA, USA), element analyzer CHNS-O UNICUBE (Elementar Analysensysteme, Frankfurt, Germany), and Melting Point M-560 (Buchi, Luzern, Switzerland) for m.p.

Shimadzu UV-1800 spectrophotometer (Shimadzu, Kyoto, Japan); Agilent Cary Eclipse spectrofluorometer (Agilent Technologies, Palo Alto, CA, USA); PalmSens analyzer (PalmSens, Enschede, The Netherlands) for cyclic voltammetry (CV); TGA Q500 device (in $N_2$ current; heating at 10° per minute; range 20–500 °C) for thermogravimetric studies (TA Instruments, Newark, DE, USA); DSC Q2000 instrument (in current $N_2$; heating at 5° per minute; interval 20–300 °C) for differential scanning calorimetry (TA Instruments, USA). The following materials (i.e., marketed reagents and solvents) were used: precursors **1**, **3**, **5**, **7**, $(Bpin)_2$, cyclooctadiene iridium chloride dimension, bis (triphenylphosphine) palladium chloride, 2,2′-bpy, tetrahydrofuran, dichloromethane, and others.

Precursor 2,6-Diborilazulene **2** was prepared according to the method [36].

### *3.1. 6-(N,N-diphenylaniline)-2-(tetramethyl-borolanyl)-azulene (**4**)*

To the mixture of 140 mg (0.43 mmol) of **3** and 491 mg (1.30 mmol) of **2** in 10 mL of degassed THF/$H_2O$ (4:1 ratio) under an argon atmosphere was added 16 mg (0.02 mmol) of $Pd(PPh_3)_2CI_2$ and 181 mg (1.30 mmol) of potassium carbonate. Then, it was boiled for 8 h at 75–80 °C. The mixture was cooled and extracted with DCM (3 × 18 mL). Then, it was dried with magnesium sulfate, and DCM was removed on a rotary evaporator (Buchi, Switzerland). The resulting substance was purified via chromatography ($SiO_2$ column, $C_6H_{12}$/DCM mixture, 9:1 ratio) and recrystallized from DCM. A total of 348 mg of dark green solid (70% yield) was obtained. M.p. 104–105.5 °C. HRMS (ESI) *m*/*z*: $C_{34}H_{33}BN0_2$ $[M + H]^+$: 498.0384, found 498.0359. Anal. calcd for $C_{34}H_{32}BN0_2$; C 82.08, H 6.48, N 2.82. Found: C 81.89, H 6.34, N 2.89. IR (ν, $cm^{-1}$): 2935, 2862, 1576, 1426, 1412, 1330, 1232, 1160, 1058, 690. $^{1}$H NMR (Figure S1. Supplementary Materials). $^{13}$C NMR (Figure S2. Supplementary Materials).

### *3.2. 6,6-Bis(N,N-diphenylaniline)-2,2-(4-(diphenylamino)phenyl)-bis-azulene (**6**)*

To the mixture of 173 mg (0.43 mmol) of **5** and 646 mg (1.30 mmol) of **4** in 12 mL of degassed THF/$H_2O$ (4:1 ratio) under an argon atmosphere, 16 mg (0.02 mmol) of $Pd(PPh_3)_2CI_2$ and 181 mg (1.30 mmol) of potassium carbonate were added. Then, it was boiled for 8 h at 75–80 °C. Then, it was cooled and extracted with DCM (3 × 18 mL), dried with magnesium sulfate, and the DCM was removed on a rotary evaporator (Buchi, Switzerland). The resulting substance was purified by chromatography ($SiO_2$ column,

mixture $C_6H_{12}$/DCM, ratio 4:1) to obtain 746 mg of brown powder (yield 76%). HRMS (ESI) *m*/*z*: $C_{74}H_{54}N_3$ $[M + H]^+$: 984.0541, found 984.0517. Anal. calcd for $C_{74}H_{53}N_3$; C 90.30, H 5.43, N 4.27. Found C 90.10, H 5.29, N 4.34. IR (ν, $cm^{-1}$): 2919, 2860, 1579, 1452, 1409, 1331, 1268, 1170, 1070, 691. $^1$H NMR (Figure S3. Supplementary Materials). $^{13}$C NMR (Figure S4. Supplementary Materials).

*3.3. 6,6,6-tris(N,N-diphenylaniline)-2,2,2-(4-(triphenylamino)-tris-azulene (***8***)*

To the mixture of 207 mg (0.43 mmol) of **7** and 940 mg (1.93 mmol) of **4** in 12 mL of degassed THF/$H_2O$ (4:1 ratio) under an argon atmosphere, 16 mg (0.02 mmol) of $Pd(PPh_3)_2CI_2$ and 270 mg (1.93 mmol) of potassium carbonate were added. Then, it was boiled for 8 h at 75–80 °C. Then, it was cooled, and extracted with DCM (3 × 18 mL), dried with magnesium sulfate, and the DCM was removed on a rotary evaporator (Buchi, Switzerland). The obtained substance was purified by chromatography ($SiO_2$ column, mixture $C_6H_{12}$/DCM, ratio 4:1) to obtain 973 mg of brown powder (yield 72%). HRMS (ESI) *m*/*z*: $C_{102}H_{73}N_4$ $[M + H]^+$: 1353.0642, found 1353.0619. Anal. calcd for $C_{102}H_{72}N_4$; C90.50, H5.36, N4.14. Found C90.30, H5.23, N4.21. IR (ν, $cm^{-1}$): 2924, 2855, 1587, 1488, 1415, 1325, 1275, 1173, 1072, 694. $^1$H NMR (Figure S5. Supplementary Materials). $^{13}$C NMR (Figure S6. Supplementary Materials).

## 4. Conclusions

In this work, for the first time, conjugated diphenylaniline-azulene co-oligomers of linear and branched structure were synthesized: 6,6-bis (N, Ndiphenylaniline)-2,2-(4-(diphenylamino) phenyl)-bis-azulene **6** and 6,6,6-tris (N, Ndiphenylaniline)-2,2,2-(4-(triphenylamino)-tris-azulene **8**. The obtained co-oligomers have a pronounced ability to absorb and emit visible light in the range of 400–700 nm.

The obtained co-oligomers possess good solubility and thermodynamic stability and have a higher HOMO compared to oligothiophenes.

The results provide a good opportunity to design new diphenylaniline-azulene-based co-oligomers for electronic and photonic applications.

**Supplementary Materials:** The following supporting information can be downloaded at: https://www.mdpi.com/article/10.3390/molecules29215041/s1, Figure S1: $^1$H NMR spectra of 6-(N,N-diphenylaniline)-2-(4,4,5,5-tetramethyl-1,3,2-dioxaborolanyl)-azulene 4; Figure S2: $^{13}$C NMR spectra of 6-(N,N-diphenylaniline)-2-(4,4,5,5-tetramethyl-1,3,2-dioxaborolanyl)-azulene 4; Figure S3: $^1$H NMR spectra of 6,6-Bis(N,N-diphenylaniline)- 2,2-(4-(diphenylamino)phenyl)-bis-azulene 6; Figure S4: $^{13}$C NMR spectra of 6,6-Bis(N,N-diphenylaniline)- 2,2-(4-(diphenylamino)phenyl)-bis-azulene 6; Figure S5: $^1$H NMR spectra of 6,6,6-tris(N,N-diphenylaniline)-2,2,2-(4-(triphenylamino)-tris-azulene 8; Figure S6: $^{13}$C NMR spectra of 6,6,6-tris(N,N-diphenylaniline)-2,2,2-(4-(triphenylamino)-tris-azulene 8; Figure S7: Thermogravimetric measurements of co-oligomers 6 and 8; Figure S8: Differential scanning calorimetry measurements of co-oligomers 6 (a) and 8 (b); Figure S9: UV–vis absorption spectra of 6 and 8. Density Functional Theory (DFT) Calculations; Table S1: Atomic coordinates of optimized geometry of 6; Table S2: Atomic coordinates of optimized geometry of 8; Cyclic voltammetry studies.

**Author Contributions:** Conceptualization, N.M.; methodology, N.M.; software, A.I. (Amantay Iskanderov) and A.I. (Ablaykhan Iskanderov); validation, N.M., A.I. (Amantay Iskanderov), A.I. (Ablaykhan Iskanderov), S.A. and S.Z.; formal analysis, A.I. (Amantay Iskanderov) and A.I. (Ablaykhan Iskanderov); investigation, N.M., A.I. (Amantay Iskanderov), A.I. (Ablaykhan Iskanderov) and S.Z.; resources, N.M.; data curation, N.M., A.I. (Amantay Iskanderov), A.I. (Ablaykhan Iskanderov), S.A. and S.Z.; writing—original draft preparation, N.M. and S.Z.; writing—review and editing, N.M. and S.A.; visualization, A.I. (Amantay Iskanderov), A.I. (Ablaykhan Iskanderov), S.A. and S.Z.; supervision, N.M. and S.A.; project administration, N.M. All authors have read and agreed to the published version of the manuscript.

**Funding:** This research is funded by the Committee of Science of the Ministry of Science and Higher Education of the Republic of Kazakhstan (Grant No. BR21882309).

**Institutional Review Board Statement:** Not applicable.

**Informed Consent Statement:** Not applicable.

**Data Availability Statement:** The data presented in the study are included in the article/Supplementary Material, further inquiries can be directed to the corresponding authors.

**Conflicts of Interest:** The authors declare no conflicts of interest.

## References


1. Zaumseil, J.; Sirringhaus, H. Electron and Ambipolar Transport in Organic Field-Effect Transistors. *Chem. Rev.* **2007**, *107*, 1296–1323. [CrossRef] [PubMed]
2. Duan, C.; Huang, F.; Cao, Y. Recent development of push–pull conjugated polymers for bulk-heterojunction photovoltaics: Rational design and fine tailoring of molecular structures. *J. Mater. Chem.* **2012**, *22*, 10416–10434. [CrossRef]
3. Lash, T.D.; El-Beck, J.A.; Ferrence, G.M. Syntheses and Reactivity of *meso*-Unsubstituted Azuliporphyrins Derived from 6-*tert*-Butyl- and 6-Phenylazulene. *J. Org. Chem.* **2007**, *72*, 8402–8415. [CrossRef] [PubMed]
4. Wakabayashi, S.; Kato, Y.; Mochizuki, K.; Suzuki, R.; Matsumoto, M.; Sugihara, Y.; Shimizu, M. Pyridylazulenes: Synthesis, Color Changes, and Structure of the Colored Product. *J. Org. Chem.* **2007**, *72*, 744–749. [CrossRef] [PubMed]
5. Amatatsu, Y. Theoretical Prediction of the $S_1-S_0$ Internal Conversion of 6-Cyanoazulene. *J. Phys. Chem. A* **2007**, *111*, 5327–5332. [CrossRef] [PubMed]
6. Peart, P.A.; Repka, L.M.; Tovar, J.D. Emerging Prospects for Unusual Aromaticity in Organic Electronic Materials: The Case for Methano [10] annulene. *Eur. J. Org. Chem.* **2008**, *28*, 2193–2206. [CrossRef]
7. Shoji, T.; Ito, S.; Toyota, K.; Yasunami, M.; Morita, N. Synthesis, Properties, and Redox Behavior of Mono-, Bis-, and Tris[1,1,4,4,-tetracyano-2-(1-azulenyl)-3-butadienyl] Chromophores Binding with Benzene and Thiophene Cores. *Chem. Eur. J.* **2008**, *14*, 8398–8408. [CrossRef]
8. Ito, S.; Kubo, T.; Morita, N.; Ikoma, T.; Tero-Kubota, S.; Kawakami, J.; Tajiri, A. Azulene-Substituted Aromatic Amines. Synthesis and Amphoteric Redox Behavior of *N*,*N*-Di(6-azulenyl)-*p*-toluidine and *N*,*N*,*N*′,*N*′-Tetra(6-azulenyl)-*p*-phenylenediamine and Their Derivatives. *J. Org. Chem.* **2005**, *70*, 2285–2293. [CrossRef]
9. Colby, D.A.; Ferrence, G.M.; Lash, T.D. Oxidative Metalation of Azuliporphyrins with Copper(II) Salts: Formation of a Porphyrin Analogue System with a Unique Fully Conjugated Nonaromatic Azulene Subunit. *Angew. Chem. Int. Ed.* **2004**, *43*, 1346–1349. [CrossRef]
10. López-Alled, C.M.; Park, S.J.; Lee, D.J.; Murfin, L.C.; Kociok-Köhn, G.; Hann, J.L.; Wenk, J.; James, T.D.; Kim, H.M.; Lewis, S.E. Azulene-based fluorescent chemosensor for adenosine diphosphate. *Chem. Commun.* **2021**, *57*, 10608–10611. [CrossRef]
11. Xin, H.; Hou, B.; Gao, X. Azulene-Based π-Functional Materials: Design, Synthesis, and Applications. *Acc. Chem. Res.* **2021**, *54*, 1737–1753. [CrossRef] [PubMed]
12. Anderson, A.G., Jr.; Steckler, B.M. Azulene. VIII. A Study of the Visible Absorption Spectra and Dipole Moments of Some 1- and 1,3-Substituted Azulenes. *J. Am. Chem. Soc.* **1959**, *81*, 4941–4946. [CrossRef]
13. Tomin, V.I.; Włodarkiewicz, A. Anti-Kasha behavior of DMABN dual fluorescence. *J. Lumin.* **2018**, *198*, 220–225. [CrossRef]
14. Nenov, A.; Borrego-Varillas, R.; Oriana, A.; Ganzer, L.; Segatta, F.; Conti, I.; Segarra-Marti, J.; Omachi, J.; Dapor, M.; Taioli, S.; et al. UV-Light-Induced Vibrational Coherences: The Key to Understand Kasha Rule Violation in *trans*-Azobenzene. *J. Phys. Chem. Lett.* **2018**, *9*, 1534–1541. [CrossRef]
15. Del Valle, J.C.; Catalán, J. Kasha's Rule: A Reappraisal. *Phys. Chem. Chem. Phys.* **2019**, *21*, 10061–10069. [CrossRef]
16. Behera, S.K.; Park, S.Y.; Gierschner, J. Dual Emission: Classes, Mechanisms, and Conditions. *Angew. Chem. Int. Ed.* **2021**, *60*, 22624–22638. [CrossRef]
17. Dunlop, D.; Ludvíková, L.; Banerjee, A.; Ottosson, H.; Slanina, T. Excited-State (Anti)Aromaticity Explains Why Azulene Disobeys Kasha's Rule. *J. Am. Chem. Soc.* **2023**, *145*, 21569–21575. [CrossRef]
18. Wang, F.; Lai, Y.-H. Conducting Azulene—Thiophene Copolymers with Intact Azulene Units in the Polymer Backbone. *Macromolecules* **2003**, *36*, 536–538. [CrossRef]
19. Wang, F.; Lai, Y.-H.; Han, M.-Y. Stimuli-Responsive Conjugated Copolymers Having Electro-Active Azulene and Bithiophene Units in the Polymer Skeleton: Effect of Protonation and p-Doping on Conducting Properties. *Macromolecules* **2004**, *37*, 3222–3230. [CrossRef]
20. Mrozek, T.; Görner, H.; Daub, J. Multimode-Photochromism Based on Strongly Coupled Dihydroazulene and Diarylethene. *J. Chem. Eur. J.* **2001**, *7*, 1028–1040. [CrossRef]
21. Dong, J.X.; Zhang, H.L. Azulene-based organic functional molecules for optoelectronics. *Chin. Chem. Lett.* **2016**, *27*, 1097–1104. [CrossRef]
22. Ou, L.; Zhou, Y.; Wu, B.; Zhu, L. The unusual physicochemical properties of azulene and azulene-based compounds. *Chin. Chem. Lett.* **2019**, *30*, 1903–1907. [CrossRef]
23. Kurotobi, K.; Kim, K.S.; Noh, S.B.; Kim, D.; Osuka, A. A Quadruply Azulene-Fused Porphyrin with Intense Near-IR Absorption and a Large Two-Photon Absorption Cross Section. *Angew. Chem. Int. Ed.* **2006**, *45*, 3944–3947. [CrossRef] [PubMed]
24. Cristian, L.; Sasaki, I.; Lacroix, P.G.; Donnadieu, B.; Asselberghs, I.; Clays, K.; Razus, A.C. Donating Strength of Azulene in Various Azulen-1-yl-Substituted Cationic Dyes: Application in Nonlinear Optics. *Chem. Mater.* **2004**, *16*, 3543–3551. [CrossRef]

25. Ito, S.; Inabe, H.; Morita, N.; Ohta, K.; Kitamura, T.; Imafuku, K. Synthesis of Poly(6-azulenylethynyl)benzene Derivatives as a Multielectron Redox System with Liquid Crystalline Behavior. *J. Am. Chem. Soc.* **2003**, *125*, 1669–1680. [CrossRef]
26. Yamaguchi, Y.; Takubo, M.; Ogawa, K.; Nakayama, K.I.; Koganezawa, T.; Katagiri, H. Terazulene Isomers: Polarity Change of OFETs through Molecular Orbital Distribution Contrast. *J. Am. Chem. Soc.* **2016**, *138*, 11335–11343. [CrossRef]
27. Nishimura, H.; Ishida, N.; Shimazaki, A.; Wakamiya, A.; Saeki, A.; Scott, L.T.; Murata, Y. Hole-Transporting Materials with a Two-Dimensionally Expanded π-System around an Azulene Core for Efficient Perovskite Solar Cells. *J. Am. Chem. Soc.* **2015**, *137*, 15656–15659. [CrossRef]
28. Zhou, Y.; Zou, Q.; Qiu, J.; Wang, L.; Zhu, L. Rational Design of a Green-Light-Mediated Unimolecular Platform for Fast Switchable Acidic Sensing. *J. Phys. Chem. Lett.* **2018**, *9*, 550–556. [CrossRef]
29. Zhou, Y.; Zhu, L. Involving Synergy of Green Light and Acidic Responses in Control of Unimolecular Multicolor Luminescence. *Chem. Eur. J.* **2018**, *24*, 10306–10309. [CrossRef]
30. Tsuchiya, T.; Higashibeppu, M.; Mazaki, Y. Synthesis and Properties of Twisted and Helical Azulene Oligomers and Azulene Based Polycyclic Hydrocarbons. *ChemistryOpen* **2023**, *12*, e202100298. [CrossRef]
31. Tsuchiya, T.; Katsuoka, Y.; Yoza, K.; Sato, H.; Mazaki, Y. Stereochemistry, Stereodynamics, and Redox and Complexation Behaviors of 2,2′ -Diaryl-1,1′ -Biazulenes. *ChemPlusChem* **2019**, *84*, 1659. [CrossRef]
32. Tsuchiya, T.; Umemura, R.; Kaminaga, M.; Kushida, S.; Ohkubo, K.; Noro, S.I.; Mazaki, Y. Paddlewheel Complexes with Azulenes: Electronic Interaction between Metal Centers and Equatorial Ligands. *ChemPlusChem* **2019**, *84*, 655. [CrossRef] [PubMed]
33. Konishi, A.; Yasuda, M. Breathing new life into nonalternant hydrocarbon chemistry: Syntheses and properties of polycyclic hydrocarbons containing azulene, pentalene, and heptalene frameworks. *Chem. Lett.* **2021**, *50*, 195. [CrossRef]
34. Shevyakov, S.V.; Li, H.; Muthyala, R.; Asato, A.E.; Croney, J.C.; Jameson, D.M.; Liu, R.S. Orbital control of the color and excited state properties of formylated and fluorinated derivatives of azulene. *J. Phys. Chem. A* **2003**, *107*, 3295. [CrossRef]
35. Rahimi, K.; Botiz, I.; Agumba, J.O.; Motamen, S.; Stingelin, N.; Reiter, G. Light absorption of poly(3-hexylthiophene) single crystals. *RSC Adv.* **2014**, *4*, 11121. [CrossRef]
36. Fujinaga, M.; Murafuji, T.; Kurotobi, K.; Sugihara, Y. Polyborylation of azulenes. *Tetrahedron* **2009**, *65*, 7115–7121. [CrossRef]
37. Wang, Z.S.; Koumura, N.; Cui, Y.; Takahashi, M.; Sekiguchi, H.; Mori, A.; Kubo, T.; Furube, A.; Hara, K. HexylthiopheneFunctionalized Carbazole Dyes for Efficient Molecular Photovoltaics: Tuning of Solar-Cell Performance by Structural Modification. *Chem. Mater.* **2008**, *20*, 3993. [CrossRef]
38. Shirota, Y.; Kageyama, H. Charge Carrier Transporting Molecular Materials and Their Applications in Devices. *Chem. Rev.* **2007**, *107*, 953. [CrossRef]
39. Ren, S.; Habibi, A.; Ni, P.; Nahdi, H.; Bouanis, F.Z.; Bourcier, S.; Clavier, G.; Frigoli, M.; Yassar, A. Synthesis and characterization of solution-processed indophenine derivatives for function as a hole transport layer for perovskite solar cells. *Dye. Pigment.* **2023**, *213*, 111136. [CrossRef]
40. Ren, S.; Wang, Z.; Zhang, W.; Ding, Y.; Yi, Z. Donor-acceptor-based organic polymer semiconductor materials to achieve high hole mobility in organic field-effect transistors. *Polymers* **2023**, *15*, 3713. [CrossRef]
41. Murphy, A.R.; Fréchet, J.M.J. Organic Semiconducting Oligomers for Use in Thin Film Transistors. *Chem. Rev.* **2007**, *107*, 1066. [CrossRef] [PubMed]
42. Brouwer, A.M. Standards for photoluminescence quantum yield measurements in solution. *Pure Appl. Chem.* **2011**, *83*, 2213–2228. [CrossRef]
43. Tsuchiya, T.; Hamano, T.; Inoue, M.; Nakamura, T.; Wakamiya, A.; Mazaki, Y. Intense absorption of azulene realized by molecular orbital inversion. *Chem. Commun.* **2023**, *59*, 10604–10607. [CrossRef] [PubMed]
44. Ren, S.; Wang, Z.; Zhang, W.; Yassar, A.; Chen, J.; Wang, S. Incorporation of diketopyrrolopyrrole into polythiophene for the preparation of organic polymer transistors. *Molecules* **2024**, *29*, 260. [CrossRef]


**Disclaimer/Publisher's Note:** The statements, opinions and data contained in all publications are solely those of the individual author(s) and contributor(s) and not of MDPI and/or the editor(s). MDPI and/or the editor(s) disclaim responsibility for any injury to people or property resulting from any ideas, methods, instructions or products referred to in the content.